



Cite this: *Environ. Sci.: Water Res. Technol.*, 2020, **6**, 166

## Mechanical degradation of polyacrylamide at ultra high deformation rates during hydraulic fracturing†

Boya Xiong, <sup>id</sup><sup>ae</sup> Prakash Purswani, <sup>d</sup> Taylor Pawlik, <sup>c</sup> Laxmicharan Samineni, <sup>c</sup> Zuleima T. Karpyn, <sup>d</sup> Andrew L. Zydney <sup>id</sup><sup>\*c</sup> and Manish Kumar <sup>id</sup><sup>\*bc</sup>

Degradation of drag reducer polyacrylamide under high volume hydraulic fracturing (HVHF) conditions alters its polymer size, distribution and chemical composition, potentially affecting the toxicity and treatability of the resulting wastewater. This study focused on a non-chemical pathway-mechanical degradation of polyacrylamide under ultra-high fluid strain conditions ( $\sim 10^7 \text{ s}^{-1}$ ) that uniquely exist during HVHF but has not yet been explored experimentally. PAM solutions were subjected to an abrupt contraction into a narrow capillary driven by a high-pressure precision pump ( $\sim 10\,000 \text{ psi}$ ). The change in polyacrylamide size distribution was evaluated by size exclusion chromatography. The peak polymer molecular weight (MW) after a single-pass through the capillary decreased from  $10^7$  to  $7 \times 10^5 \text{ Da}$  at deformation rate  $\frac{V}{R} = 4 \times 10^6 \text{ s}^{-1}$ . The extent of degradation increased with  $\frac{V}{R}$ , approximately following an empirical scaling relationship of  $\text{MW} \propto \frac{V}{R}^{-0.69}$  for the polyacrylamide with an initial  $\text{MW} \approx 10^7 \text{ Da}$ . Degraded PAM with lower MW ( $< 10^6 \text{ Da}$ ) showed minimal degradation during multiple flow passes even at high deformation rates, suggesting that most mechanical degradation occurs at the first entrance into the fracture. Relative to chemical degradation, mechanical degradation caused a narrowing of the MW distribution due to greater degradation of the larger MW polymers and preferential mid-chain polymer scission. In addition, we saw no detectable change in chemical composition during mechanical scission, in contrast to the generation of carbonyl groups during oxygenic radical induced chemical degradation. Combining both chemical and mechanical mechanisms during HVHF operation, we propose an initial mechanical breakage of polymer chain by fluid strain, followed by chemical degradation under the high temperature and appropriate mineralogical conditions. These findings provide critical information for understanding the nature of degradation byproducts from polyacrylamide, and the treatability of polyacrylamide fragment-containing wastewaters.

Received 23rd June 2019,  
Accepted 11th November 2019

DOI: 10.1039/c9ew00530g

rsc.li/es-water



### Water impact

Here we explore a non-chemical mechanism-mechanical degradation of polyacrylamide under ultrahigh shear rates unique to high volume hydraulic fracturing operations. The fundamental understanding enables us to estimate the extent and chemistry of degradation given geological and operational conditions. Such estimation will facilitate fracturing fluid chemists, well operators and regulators to manage chemical usage, characterize and treat fracturing wastewaters, and mitigate risks of environmental releases.

<sup>a</sup> Department of Civil and Environmental Engineering, Massachusetts Institute of Technology, USA. E-mail: boyax@mit.edu

<sup>b</sup> Department of Civil and Environmental Engineering, The Pennsylvania State University, USA. E-mail: manish.kumar@psu.edu

<sup>c</sup> Department of Chemical Engineering, The Pennsylvania State University, USA. E-mail: zydney@engr.psu.edu

<sup>d</sup> John and Willie Leone Family Department of Energy and Mineral Engineering, The Pennsylvania State University, USA

<sup>e</sup> Department of Civil, Environmental and Geo-Engineering, University of Minnesota, Minneapolis, MN 55455, USA. E-mail: bxiong@umn.edu

† Electronic supplementary information (ESI) available: High shear rate capillary flow setup images, power law fluid parameters calculation, estimation of shear rates in actual hydraulic fracturing operations are included in the ESI. See DOI: 10.1039/c9ew00530g

### Introduction

The fate of hydraulic fracturing chemicals when injected into the deep subsurface is still poorly understood, yet they strongly impact the resulting wastewater quality and thus the possible environmental impact of accidental spills or storage pond leakages of wastewater. Chemical and biological transformations of these chemicals have been previously discussed;<sup>1–3</sup> mechanical degradation is an additional pathway that could be of significant importance to high molecular weight (MW) polymer chemicals. During HVHF operations, fluids containing ultrahigh MW polyacrylamide

(PAM) ( $2 \times 10^7$  Da) are pumped at high flow rates down through the wellbore and into tight shale formations, creating highly permeable fractures under high hydraulic pressure (up to 10 000 psi (ref. 4)). Long-chain PAM acts as a friction reducer, suppressing turbulent vortices and thereby reducing pumping cost.<sup>5,6</sup> Low levels of mechanical chain scission can occur under low strain rates ( $<10^5$  s<sup>-1</sup>), similar to those encountered during flow through valves, pipes, and the wellbore, decreasing the polymer MW and lowering the degree of drag reduction.<sup>7</sup>

Previous studies have demonstrated the loss in viscosity and drag reduction for dilute and semi-dilute PAM solutions due to chain rupture in both laminar and turbulent extensional flow, *e.g.*, upon flow into an abrupt or tapered contraction.<sup>8-15</sup> PAM degradation has also been observed in porous media, but this might not be applied in the context of HVHF due to limited transport of hundred-nanometer size polymer coils into the nano- to micro-Darcy range pores in tight shale formations.<sup>16,17</sup> Most studies have only focused on evaluating changes in viscosity, with no detailed information presented on the actual changes in polymer molecular size distribution and chemical composition.<sup>18</sup> However, the polymer molecular size distribution was found to be determine the fouling potential during wastewater treatment using microfiltration membranes;<sup>19</sup> and chemical composition is critical in estimating the persistence, mobility and toxicity of degraded molecules in wastewater.<sup>20</sup> Limited estimates of MW changes have been reported using the Mark-Houwink-Sakurada equation but the accuracy of this approach is questionable due to the large variation of the model coefficients with MW distribution, chemical structure, and the presence of solution impurities.<sup>21</sup>

Capillary flow geometry has previously been utilized to study polymer degradation in reservoir flow,<sup>10,22</sup> and can potentially better simulate hydraulically stimulated fracture flow. Such flow with an abrupt contraction entrance contains shear and extensional fluid component,<sup>23</sup> both of which contribute to fluid stress but seem to play different roles in polymer scission. In particular, the extensional flow at such geometry is transient instead of quasi-steady state stagnant (as encountered in cross-slot geometry), under which coiled polymer chain only partially extend.<sup>24</sup> Jouenne *et al.*<sup>22</sup> compared the extent of PAM degradation (determined from the change in viscosity) in a capillary constriction, porous media, and a blender. Degradation was found to be governed by the extensional flow at the capillary entrance instead of the wall shear inside the capillary tube, as data obtained with capillaries of different length showed the same degree of degradation when plotted in terms of the flow rate (and not the pressure drop). In addition, the extent of degradation increased with increasing time (in the blender) and with increasing number of passes (for flow into the capillary), approaching an asymptote after extended exposure/passes. Vanapalli *et al.* developed a turbulence theory based scaling correlation that can be applied to a variety of flow geometries including abrupt contraction.

Such scaling correlation explains, in addition to extensional flow stress, scission of extended polymer chain is also likely caused by the fluid tension from velocity fluctuation at Kolmogorov scale of turbulence.<sup>25</sup> However, these experiments were limited to very low shear rates ( $<10^5$  s<sup>-1</sup>), with no information provided on the nature of the polymer breakage. Buchholz *et al.*<sup>26</sup> showed that scission of high MW polymers occurs preferentially near the chain mid-point and for larger MW species (in turbulent flow), leading to a decrease in polydispersity as determined by gel permeation (size exclusion) chromatography.<sup>26</sup> During HVHF, flow through perforations/fractures during the initial fracture will create high levels of pressures and shear rates, likely creating strain rates well in excess of  $10^5$  s<sup>-1</sup>, a flow regime that has yet to be investigated for the mechanical degradation of PAM.

The objective of this study was to first examine the mechanical degradation of high MW PAM after flow through a sharp contraction into very narrow capillaries at the high pressures/shear rates that would be expected during the HVHF of tight shale formations. In each case, the degree of degradation was evaluated using the change in polymer MW distribution quantified by size exclusion chromatography both before and after flow through narrow capillaries. The MW distribution of degraded polymer was then used to establish a scaling relationship with the applied shear rates. Second, mechanical degradation was compared to chemical degradation of PAM under HVHF chemical conditions (high temperature, mg L<sup>-1</sup> level Fe<sup>2+</sup> at pH < 4) in terms of MW distribution and chemical functional groups of degraded polymer. Furthermore, sequential and combined degradation experiments by the two mechanisms were performed and the degree of degradation was quantified. The results presented here provides a holistic view of PAM degradation throughout the HVHF process by both chemical and mechanical mechanisms.

## Methods

### Commercial PAM solution and analysis

PAM solutions were prepared at a concentration of 1.5% v/v using a commercial friction reducer formulation described previously.<sup>27</sup> In order to prevent potential clogging, polymer solutions were prefiltered through a Whatman® Grade 3 filter paper with a pore size of 6 µm. The kinematic viscosity of this polymer solution was  $8 \times 10^{-6}$  m<sup>2</sup> s<sup>-1</sup> as determined with a CANNON-Fenske viscometer (size 75, 20 °C). Original and degraded polymer solutions were analyzed by size exclusion chromatography using a method described previously.<sup>27</sup> To further characterize the chemical structure change during mechanical degradation, attenuated total reflectance-Fourier transform infrared spectroscopy (ATR-FTIR) was performed using methods and procedures described previously.<sup>27</sup> Raw fracturing fluid and flowback were dried on a hotplate at 50 °C into solid powder before analyses.



## High-shear rate capillary flow set up

High shear rate capillary flow experiments were performed using the apparatus shown in Fig. S1A and B.† The selected capillary diameters and applied pressures were chosen to provide a shear range of  $10^5$ – $10^7$  s $^{-1}$ , simulating the high range of shear rates during HVHF that has not been investigated previously. To the best of our knowledge, these shear rates in actual HVHF operations have not been estimated previously in the literature, and we calculated shear rates within the range from  $10^3$ – $10^8$  s $^{-1}$  using eqn (S-11) and (S-12)† and midrange literature values of operation and well specifics listed in Table S2.† Note that we do not intend to use the capillary diameters and pressures in our experiments to simulate fracture or perforation diameters or net pressure (that drives fracture propagation), as only the resulting shear rates were used to build the scaling relationship for estimating polymer degradation.

This apparatus consists of a high precision metering pump (Quizix® Q5000-10 K, rated as 10 000 psi, 15 ml min $^{-1}$  max flow rate, Chandler Engineering), PEEKsil® capillary tubing (SGE analytical service by Trajan Scientific and Medical, Australia) connected by EXP® 2 titanium hybrid Ti-LOK ferrule (#15-20-04932, Optimize Technologies, OR) and standard reducing union (# ZRU21 T, VICI Valco® Instruments, TX); all parts were rated at a pressure of at least 15 000 psi. The capillary tubing had a polymer outer sheath (polyether ether ketone, PEEK), a polyimide layer in the middle, and a fused silica lining inside to provide very low adsorption characteristics. Experiments were performed with capillaries having inner-diameters of 50 and 75  $\mu\text{m}$ , with an outer-diameter of 1.5875 mm (1/16").

Experiments were conducted at constant flow rate (determined by timed collection of the outflow) with the pressure recorded using Quizix® PumpWorks software. Samples (20 mL) were collected from the system outflow (after pressure equilibration, roughly 10 min) for offline determination of the PAM MW distribution. Linearized flow rate and pressure data were plotted to calculate the power law fluid index  $n$  and consistency factor  $K$ , which were then used to calculate shear rate,  $\dot{\gamma}_v = \left(\frac{3n+1}{n}\right) \frac{V}{R}$ , where  $V$  is the mean flow velocity and  $R$  is the capillary radius. Characteristic strain rate that represents the extensional component was calculated as  $\dot{\epsilon} = 0.56 \frac{V}{R}$  that was previously developed for sharp-contraction capillary flow.<sup>11</sup> Thus, the shear rate and strain rate both have the same dependence on the fluid velocity and capillary radius in this system, making it very difficult to separate out the contributions of shear *versus* elongational flow on the extent of degradation. Therefore, we use  $V/R$  as the independent variable to represent the overall deformation rate of the fluid under such geometry and was used to establish the scaling relationship between fluid strain rate and molecular weight reduction. Note that the both  $\dot{\gamma}_v$  and  $\dot{\epsilon}$  are linearly proportional to  $V/R$ .

## Chemical and mechanical degradation

The effects of simultaneous chemical and mechanical degradation were examined by heating the connecting tubes between the pump and the capillary with high-temperature heating tapes to achieve a temperature of 80 °C at the capillary entrance. The residence time in the connecting tube was ~3 min. Temperature was monitored by a surface thermometer (wrapped inside of the heating tape along the outer surface of the capillary) and by a portable digital thermometer that was used to measure the temperature of the fluid entering the capillary. The reservoir polymer solution was kept at room temperature to minimize chemical degradation prior to the flow contraction. Chemical degradation conditions were achieved by adding 200 mM Fe $^{2+}$  stock solution (dissolved in 0.2 M HCl) and 0.5 M HCl to the polymer solution to yield a final Fe $^{2+}$  concentration of 2 mg L $^{-1}$  and a pH of 3.5.<sup>27</sup> Experiments were performed in the following sequence: (1) polymer solution without Fe $^{2+}$  flow through a capillary ("Mech"); (2) polymer solution with Fe $^{2+}$  without capillary ("Chem"); (3) polymer solution with Fe $^{2+}$  flow through a capillary ("Chem + Mech"); (4) polymer solution without Fe $^{2+}$  first flowed through a capillary then Fe $^{2+}$  added ("Mech + Chem"). (5) Solution from experiment (4) flowed through a capillary again ("Mech + Chem + Mech"). All the experiments were performed in duplicate in single pass flow experiments.

## Results and discussion

### Impact of shear rate on degradation during single flow pass

Molecular size reduction of PAM after flow into the narrow capillaries (with deformation rates from  $10^5$  to  $4 \times 10^6$  s $^{-1}$ , shear rate from  $10^5$  to  $10^7$  s $^{-1}$ ) was determined by size exclusion chromatography. The peak MW of PAM was largely unchanged after flow into the capillary at  $V/R < 10^5$  s $^{-1}$  (shear rates  $\dot{\gamma}_v < 10^6$  s $^{-1}$ ), but there was more than one order of magnitude reduction in peak MW after flow into the capillary at a  $V/R = 1.5 \times 10^6$  s $^{-1}$  (shear rate  $\dot{\gamma}_v = 2 \times 10^7$  s $^{-1}$ ) (Fig. 1A). All shear rates were calculated using the power law fluid index  $n = 1.008 \pm 0.025$  ( $\tau = Ky^n$ ) determined from a log-log plot of pressure *versus* flow rate (Table S1†). This value of  $n$  suggests that the flow was nearly Newtonian at the very high shear rates examined in this work. In addition, the strength of extensional flow component was calculated as the characteristic strain rate ( $\dot{\epsilon}$ ); the shear and strain rate of flow experiments with 75  $\mu\text{m}$  capillary was presented in Table S1.† The data for the peak MW for the 50 and 75  $\mu\text{m}$  capillary diameters appeared to be very similar, although the same trend was also seen when plotting the peak MW *versus* the average flow velocity in the capillary as suggested by Jouenne *et al.*<sup>22</sup> The relationship between resulting MW with  $V/R$  was plotted on a log-log graph, suggesting a correlation of the form:

$$\text{MW} \propto \frac{V^{-0.69}}{R}, \quad (1)$$



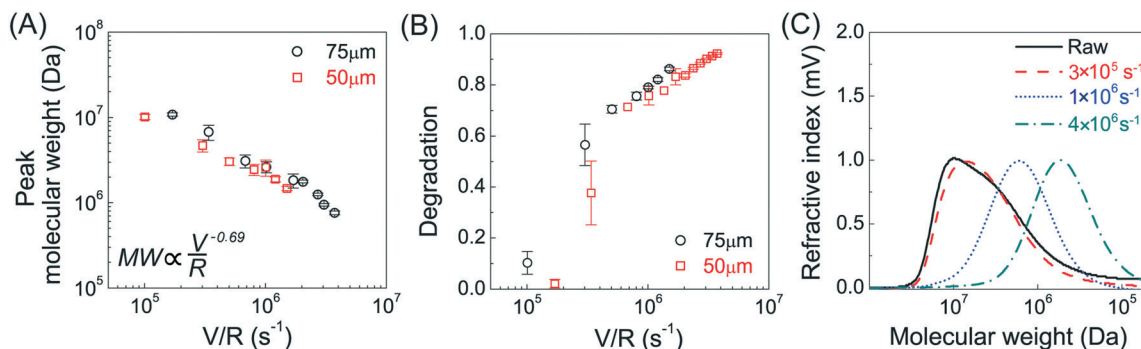


**Fig. 1** (A) The peak molecular weight of PAM as a function of  $V/R$  for a single pass through 50 and 75  $\mu\text{m}$  capillaries. The data represent the average value for triplicate experiments. (B) The percent degradation of PAM calculated as a shift from the initial MW after passing through the capillaries at higher  $V/R$ . (C) Size exclusion chromatographs of polymer after flow through 50  $\mu\text{m}$  capillary at different  $V/R$  values. The height of the peaks were normalized to the maximum peak height to facilitate comparison.

although this result is specific for the large MW PAM examined in this study. The power law relationship for shear rate and characteristic strain rate is same as  $V/R$  (e.g.,  $MW \propto \dot{\varepsilon}^{-0.69}$ ). Similar power-law relationships have been reported for polystyrene solution in transient abrupt contraction flow,<sup>28</sup> polyethylene oxide and polyacrylamide solution in turbulent pipe flow,<sup>7</sup> where the scaling exponent was found to range between 0.36–1. Such correlation reflects the critical fluid strength that is needed for chain rupture under specific flow geometry. This can be better seen in Fig. 1B, which is re-plotted using the data in Fig. 1A as the percent degradation, defined as the reduction in the peak MW divided by the initial MW. There was no degradation for the experiments with  $V/R$  below  $10^5$   $s^{-1}$ , suggesting that there is a critical fluid strain (or stress) needed to initiate the scission of the polymer chain. The percent degradation drastically increased after flow into capillaries at high deformation rates (Fig. 1B), as evident from the size exclusion chromatographs (Fig. 1C). In addition, the breadth of the MW distribution decreased after mechanical degradation, consistent with the preferential scission of the larger MW species near the middle of the polymer chain.

### Degradation during multiple flow passes

Branched fractures are likely to form during hydraulic fracture propagation, introducing polymer to multiple flow events into narrow fractures.<sup>29</sup> To investigate the effects of multiple exposure of PAM to high deformation rates, we conducted multiple cycles of mechanical degradation. The polymer solution was collected from the outlet of the 75  $\mu\text{m}$  capillary and then pumped through the capillary again, with this process repeated 20 times. The measured peak MW for each pass through the capillary (at a  $V/R$  of  $1.2 \times 10^6$   $s^{-1}$ ) is shown in Fig. 2A. Most of the degradation ( $\sim 90\%$ ) occurred during the first pass, with a small decrease in peak MW after each of the repeated pump passes. The final peak MW after 20 pump passes was  $7 \times 10^5$  Da compared to the initial value of  $10^7$  Da. Note that no change in MW was observed in the control experiment where the polymer solution was passed repeatedly through the pump, tubing, and fittings but without the capillary/constriction. Re-plotting the data as the percent degradation as a function of the inlet (feed) MW (Fig. 2B) highlights the presence of a critical polymer size ( $MW \approx 7 \times 10^5$  Da) below which there is no further degradation under these conditions (corresponding to a  $V/R$  of  $1.2 \times 10^6$   $s^{-1}$ ).

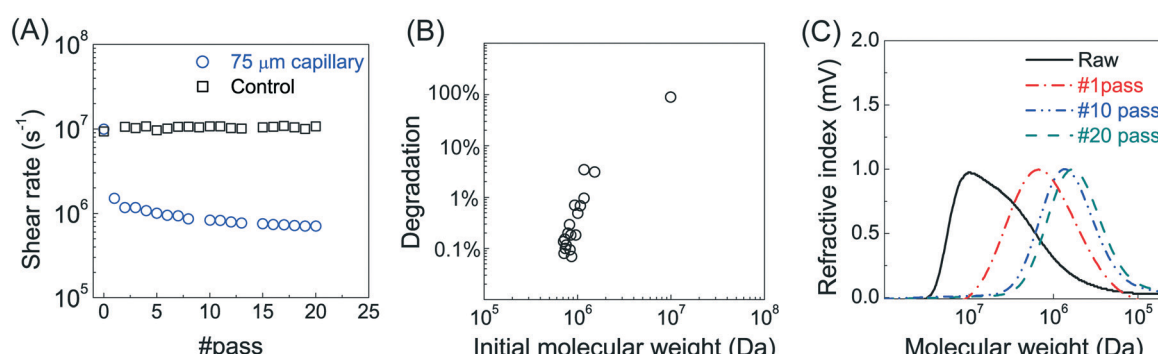


**Fig. 2** (A) Peak MW decreases after repeated passes through the 75  $\mu\text{m}$  capillary. Results are average of two repeated sets of experiments. (B) Percent degradation as a function of the initial peak MW of the polymer for each pass. (C) Size exclusion chromatographs of polymer solution after the 1st, 10th, and 20th pass.



Our data demonstrate that a stronger extensional flow (corresponding to a higher capillary deformation rate) is required to break a shorter polymer chain (low MW), which is consistent with previous studies suggesting a critical (minimum) polymer size for chain scission under given flow conditions.<sup>22,26</sup> It was suggested that a larger polymer chain is more likely to be deformed under strain due to 1) decreased molecular mobility (characterized by relaxation time), 2) a higher capacity of storing elastic energy by strain accumulation.<sup>28</sup> This further highlights the importance of the power law scaling relationship under such flow regime ( $MW \propto \frac{V}{R}^{-0.69}$ ). As a result, the highest level of reduction in both the peak MW and polydispersity occurs at the first passage of the polymer through the highly contracting capillary (Fig. 2C), which is likely to reflect the degradation during the fracture initiation phase during HVHF operations. Subsequent flow through the fracture, including entrance to branched fractures, are likely to have lower shear rates due to pressure loss and leak off during fracture flow;<sup>30,31</sup> thus, the subsequent degradation would be much less than the breakage seen during the entrance to the initial fracture.

### Chemical versus mechanical degradation

Deep subsurface conditions during hydraulic fracturing provide a unique environment where PAM can undergo significant chemical degradation due to the presence of oxygenic free radicals.<sup>20</sup> Therefore, an additional series of experiments was performed with the PAM solution mixed with 2 mg L<sup>-1</sup> Fe<sup>2+</sup> (pH 3.5, 8 ppm dissolved oxygen) at a temperature of 80 °C, and single pass through capillary flow at a V/R of 1.2 × 10<sup>6</sup> s<sup>-1</sup>, to evaluate the effects of chemical and mechanical degradation, both separately and in combination (Fig. 3A). Chemical degradation alone caused about a 1.7-fold reduction in MW compared to the more than

3-fold reduction due to mechanical degradation alone, although previous studies have demonstrated that there will be significantly more chemical degradation after longer time exposure (>24 h) to the oxygen radicals at these low pH conditions.<sup>27</sup> The combination of mechanical and chemical degradation caused more than a 4-fold reduction in MW, with the final MW being slightly smaller when the mechanical degradation was followed by chemical degradation. For example, chemical degradation first led to a reduction in MW to 5 × 10<sup>6</sup> Da, with the capillary flow degrading the polymer further to MW = 2.0 × 10<sup>6</sup> Da compared to a final MW of 1.7 × 10<sup>6</sup> Da for mechanical followed by chemical degradation.

The differences in chemical and mechanical degradation were further studied using attenuated total reflectance Fourier transform infrared spectroscopy (ATR-FTIR). Mechanically degraded PAM had a similar FTIR spectrum as compared to the original polymer. In comparison, the chemically degraded polymer showed a distinct signal associated with the carbonyl group (peak at 1720 cm<sup>-1</sup> in Fig. 3B). The carbonyl group generated during chemical degradation is due to the  $\beta$ -scission of peroxy radical subsequent to the oxygen radical attack on the polymer chain,<sup>27</sup> a phenomenon that does not occur during the C-C bond breakage by mechanical forces.

The polydispersity index (PDI) of the PAM decreased significantly after either mechanical or chemical degradation (Fig. 3C). The PDI for each polymer was calculated as the ratio of the weight average molecular weight (M<sub>w</sub>) to the number average molecular weight (M<sub>n</sub>) as determined from the size exclusion chromatographs using appropriate calibration curves (created with PAM standards having a range of molecular weights). We selected a chromatograph from a previous study of chemical degradation<sup>27</sup> with similar peak MW to better visualize the PDI comparison for the various degradation mechanisms. Mechanical degradation

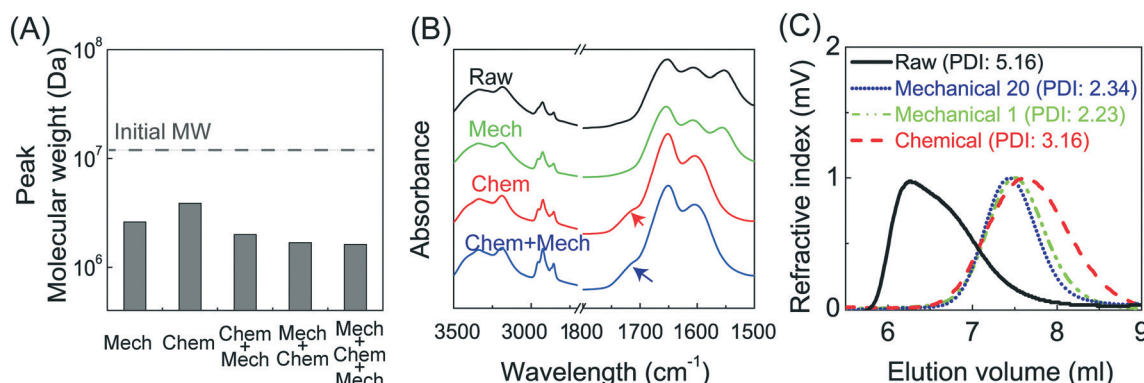


Fig. 3 A) Effect of mechanical and chemical degradation on PAM. "Mech" indicates solution with just polymer that passes through a 75  $\mu$ m capillary at a V/R of  $1.2 \times 10^6$  s<sup>-1</sup>; all the samples with "Chem" indicate solutions of polymer mixed with 2 ppm Fe<sup>2+</sup> at a pH 3.5. The order of "Mech" and "Chem" indicates the order of the experiment. B) FTIR spectra of raw, chemically, mechanically, and combined degraded polymer shows an increase in the carbonyl groups only after chemical degradation (arrows). (C) Chromatographs of raw, mechanically, and chemically degraded polymer with similar peak MW suggest a stronger PDI-narrowing capability of mechanical degradation. The chromatograph of the chemically degraded polymer was extracted from a previous study where the polymer was degraded for 14 h in the presence of outcrop shale at 80 °C.<sup>27</sup>



led to a narrower molecular weight distribution (smaller PDI in Fig. 3C) compared to chemical degradation, consistent with the physical picture that mechanical forces lead to the preferential breakage of the larger MW polymers near the midpoint of the chain.<sup>26</sup> In contrast, chemically generated free radicals are likely to attack randomly along the entire polymer chain length, irrespective of the initial polymer MW. Mechanical degradation is less effective in reducing the peak MW when it follows chemical degradation since much of the chemically-degraded PAM will have low MW (below the critical MW for polymer chain scission) and will thus be unaffected by the extensional flow. In contrast, chemical degradation will be highly effective in further degrading the PAM that has already been subjected to the extensional flow. Note that previous studies of chemical degradation yielded PAM with peak MW below  $2 \times 10^5$  Da after 24 h exposure to  $\text{Fe}^{2+}$ -generated hydroxyl radicals at low pH and high temperatures,<sup>20</sup> which is well below the lowest MW seen in this study after multiple sequential mechanical degradation events.

## Engineering implications

Here we further describe the flow events and calculate the shear rate (as a representation of the fluid strength) range during an actual HVHF operation, in order to estimate the degree of mechanical degradation of PAM using the scaling relationship developed in this work. During the fracture initiation phase, polymer fluid is vigorously pumped through millimeter size perforations in the shale formation. We estimated the shear rate of flow through perforations with 0.005–0.02 m diameter and 0.2–1.0 m depth at a pumping rate of 55 bbl min<sup>-1</sup> and net pressure of 200–2000 psi (note that the net pressure is the difference between wellbore pressure and *in situ* horizontal stress of shale). The associated literature values, assumptions, and equations are presented in Table S2.† Simply flowing through the perforation yields a maximum shear rate of  $10^5$  up to  $10^8$  s<sup>-1</sup> (Table S3†), which is comparable to the shear rates/extensional flow rates encountered in the capillaries used in this study. The maximum shear rate of  $10^8$  s<sup>-1</sup> can result in significant PAM degradation, resulting in a peak MW of  $<10^5$  Da, according to the scaling relationship of  $\text{MW} \propto \dot{\gamma}_v^{-0.69}$  established here.

In addition, shale formations with high ferrous-bearing minerals can utilize oxygen in the fluid to generate oxygenic radicals that can cause further chemical degradation of PAM. Combined chemical and mechanical degradation results also suggest distinct features of the two mechanisms which suggests that each mechanism is likely to dominate at different stages of fracturing events. Mechanical degradation is likely to be dominant at the entrance of fracture when polymer MW is still high (above critical chain length for scission) and chemical degradation is not fast enough to occur (milli-second for mechanical degradation *versus* minute to hour for chemical degradation). Once inside the fracture,

mechanically degraded polymer chains are likely to be chemically degraded, where chain scission occurs randomly along the polymer chain, generating carbonyl groups *via*  $\beta$ -scission that are absent in both the raw and mechanically degraded polymer.

## Conclusion

For the first time, we have quantified the significant MW reduction of polyacrylamide by mechanical degradation mechanism under high shear rate conditions ( $\dot{\gamma}_v \sim 10^5$ – $10^7$  s<sup>-1</sup>;  $\frac{V}{R} \sim 10^5$ – $4 \times 10^6$ ) unique to HVHF operations. Log-log scaling relationship between final MW of polyacrylamide and fluid deformation rate was developed  $(\text{MW} \propto \frac{V}{R}^{-0.69})$ . This relationship enables the estimation of the maximal three orders of magnitude of MW reduction (with a starting MW of  $10^7$  Da) under a shear rate of  $10^8$  s<sup>-1</sup>. Mechanical degradation leads to a decrease in polydispersity of PAM suggesting preferred scission at mid-chain compared to random chain scission of chemical degradation. Furthermore, mechanically degraded PAM is chemically similar to un-degraded PAM, compared to carbonyl group generation during chemical degradation by  $\beta$ -scission of oxyl radicals. The combination of mechanical and chemical degradation introduces PAM with a wide range of MW distribution in the wastewater. Largely degraded polymer can contribute significantly to the polar organic fraction in the wastewater and enhance the likelihood of releasing hazardous acrylamide monomer into the environment. Polymer debris with low degree of degradation can significantly increase the fouling potential during the membrane treatment of the resulting wastewater. This work provides mechanistic insights into the unique transformation pathway of polyacrylamide in the deep subsurface and justify the need for more detailed chemical and toxicological analyses of degraded polymer products in HVHF wastewaters.

## Conflicts of interest

The authors declare no competing financial interest.

## Acknowledgements

Partial support for this work was provided by a Penn State College of Engineering Innovation Grant and a seed grant through the Center for Collaborative Research in Intelligent Gas Systems (CCRINGS) program funded by General Electric (GE). Additional support was provided by the Pennsylvania Water Resources Research Center small grants program.

## References

- 1 A. J. Sumner and D. L. Plata, Halogenation chemistry of hydraulic fracturing additives under highly saline simulated subsurface conditions, *Environ. Sci. Technol.*, 2018, 52(16), 9097–9107.



2 R. A. Daly, M. A. Borton, M. J. Wilkins, D. W. Hoyt, D. J. Kountz and R. A. Wolfe, *et al.* Microbial metabolisms in a 2.5-km-deep ecosystem created by hydraulic fracturing in shales, *Nat. Microbiol.*, 2016, **1**, 16146.

3 J. Rosenblum, E. M. Thurman, I. Ferrer, G. Aiken and K. G. Linden, Organic chemical characterization and mass balance of a hydraulically fractured well: from fracturing fluid to produced water over 405 days, *Environ. Sci. Technol.*, 2017, **51**(23), 14006–14015.

4 A. J. Sumner and D. L. Plata, Exploring the hydraulic fracturing parameter space: a novel high-pressure, high-throughput reactor system for investigating subsurface chemical transformations, *Environ. Sci.: Processes Impacts*, 2018, **20**(2), 318–331.

5 H. Usui, M. Kodama and Y. Sano, Laser-Doppler measurements of turbulence structure in a drag-reducing pipe flow with polymer injection, *J. Chem. Eng. Jpn.*, 1988, **21**(2), 134–140.

6 T. Rho, J. Park, C. Kim, H.-K. Yoon and H.-S. Suh, Degradation of polyacrylamide in dilute solution, *Polym. Degrad. Stab.*, 1996, **51**(3), 287–293.

7 S. A. Vanapalli, M. T. Islam and M. J. Solomon, Scission-induced bounds on maximum polymer drag reduction in turbulent flow, *Phys. Fluids*, 2005, **17**(9), 095108.

8 A. H. Abdel-Alim and A. E. Hamielec, Shear degradation of water-soluble polymers. I. Degradation of polyacrylamide in a high-shear couette viscometer, *J. Appl. Polym. Sci.*, 1973, **17**(12), 3769–3778.

9 J. M. Maerker, Shear degradation of partially hydrolyzed polyacrylamide solutions, *Soc. Pet. Eng. J.*, 1975, **15**(04), 311–322.

10 A. Zaitoun, P. Makakou, N. Blin, R. S. Al-Maamari, A.-A. R. Al-Hashmi and M. Abdel-Goad, Shear stability of EOR polymers, *SPE J.*, 2012, **17**(02), 335–339.

11 A. B. Metzner and A. P. Metzner, Stress levels in rapid extensional flows of polymeric fluids, *Rheol. Acta*, 1970, **9**(2), 174–181.

12 A. F. Horn and E. W. Merrill, Midpoint scission of macromolecules in dilute solution in turbulent flow, *Nature*, 1984, **312**(5990), 140.

13 J. D. Culter, J. L. Zakin and G. K. Patterson, Mechanical degradation of dilute solutions of high polymers in capillary tube flow, *J. Appl. Polym. Sci.*, 1975, **19**(12), 3235–3240.

14 D. Hunkeler, T. Q. Nguyen and H. H. Kausch, Polymer solutions under elongational flow: 2. An evaluation of models of polymer dynamics for transient and stagnation point flows, *Polymer*, 1996, **37**(19), 4271–4281.

15 B. R. Elbing, E. S. Winkel, M. J. Solomon and S. L. Ceccio, Degradation of homogeneous polymer solutions in high shear turbulent pipe flow, *Exp. Fluids*, 2009, **47**(6), 1033–1044.

16 B. Bazin, S. Bekri, O. Vizika, B. Herzhaft and E. Aubry, Fracturing in tight gas reservoirs: application of special-core-analysis methods to investigate formation-damage mechanisms, *Soc. Pet. Eng. J.*, 2010, **15**(04), 969–976.

17 S. A. Holditch, Tight gas sands, *JPT, J. Pet. Technol.*, 2006, **58**(06), 86–93.

18 Modeling viscosity and mechanical degradation of polyacrylamide solutions in porous media, *SPE Improved Oil Recovery Conference*, ed. K. Brakstad and C. Rosenkilde, Society of Petroleum Engineers, 2016.

19 B. Xiong, S. Roman-White, B. Piechowicz, Z. Miller, B. Farina and T. Tasker, *et al.* Polyacrylamide in hydraulic fracturing fluid causes severe membrane fouling during flowback water treatment, *J. Membr. Sci.*, 2018, **560**, 125–131.

20 J. D. Rogers, T. L. Burke, S. G. Osborn and J. N. Ryan, A Framework for Identifying Organic Compounds of Concern in Hydraulic Fracturing Fluids Based on Their Mobility and Persistence in Groundwater, *Environ. Sci. Technol. Lett.*, 2015, **2**(6), 158–164.

21 K. C. Tam, C. Tiu and T. N. Fang, Comments on the accuracy of zero shear intrinsic viscosity of high molecular weight polyacrylamide, *Polym. Int.*, 1991, **24**(1), 15–22.

22 S. Jouenne, H. Chakibi and D. Levitt, Polymer stability after successive mechanical-degradation events, *Soc. Pet. Eng. J.*, 2018, **23**(01), 18–33.

23 P. Schunk and L. Scriven, Constitutive equation for modeling mixed extension and shear in polymer solution processing, *J. Rheol.*, 1990, **34**(7), 1085–1119.

24 T. Q. Nguyen and H.-H. Kausch, Mechanochemical degradation in transient elongational flow, *Macromolecules: Synthesis, Order and Advanced Properties*, Springer, 1992, pp. 73–182.

25 S. A. Vanapalli, S. L. Ceccio and M. J. Solomon, Universal scaling for polymer chain scission in turbulence, *Proc. Natl. Acad. Sci. U. S. A.*, 2006, **103**(45), 16660–16665.

26 B. A. Buchholz, J. M. Zahn, M. Kenward, G. W. Slater and A. E. Barron, Flow-induced chain scission as a physical route to narrowly distributed, high molar mass polymers, *Polymer*, 2004, **45**(4), 1223–1234.

27 B. Xiong, Z. Miller, S. Roman-White, T. Tasker, B. Farina, B. Piechowicz, W. D. Burgos, P. Joshi, L. Zhu, C. A. Gorski and A. L. Zydny, Chemical degradation of polyacrylamide during hydraulic fracturing, *Environ. Sci. Technol.*, 2018, **52**(1), 327–336.

28 T. Q. Nguyen and H.-H. Kausch, Chain extension and degradation in convergent flow, *Polymer*, 1992, **33**(12), 2611–2621.

29 S. Rahimi-Aghdam, V.-T. Chau, H. Lee, H. Nguyen, W. Li and S. Karra, *et al.* Branching of hydraulic cracks enabling permeability of gas or oil shale with closed natural fractures, *Proc. Natl. Acad. Sci. U. S. A.*, 2019, **116**(5), 1532–1537.

30 Montgomery MBSaCT, *Hydraulic fracturing*, CRC Press Taylor & Francis Group, 2015.

31 Fracturing fluid leakoff under dynamic conditions part 2: Effect of shear rate, permeability, and pressure, *SPE Annual Technical Conference and Exhibition*, ed. S. Vitthal and J. McGowen, Society of Petroleum Engineers, 1996.

